ARTICLE
Journal of Cellular Biochemistry 117:207–217 (2016)

Journal of Cellular Biochemistry

Functional Analysis of *GLRX5* Mutants Reveals Distinct Functionalities of GLRX5 Protein

Gang Liu,[1] Yongwei Wang,[1,2] Gregory J. Anderson,[3] Clara Camaschella,[4] Yanzhong Chang,[2] and Guangjun Nie[1]*

[1]*CAS Key Laboratory for Biomedical Effects of Nanomaterials and Nanosafety, National Center for Nanoscience and Technology, No.11 Zhongguancun Beiyitiao, Beijing 100190, China*

[2]*Laboratory of Molecular Iron Metabolism, College of Life Science, Hebei Normal University, Shijiazhuang 050024, Hebei Province, China*

[3]*Iron Metabolism Laboratory, QIMR Berghofer Medical Research Institute, Brisbane, Queensland, Australia*

[4]*Vita-Salute University, and IRCCS San Raffaele Scientific Institute, Milan, Italy*

ABSTRACT

Glutaredoxin 5 (GLRX5) is a 156 amino acid mitochondrial protein that plays an essential role in mitochondrial iron-sulfur cluster transfer. Mutations in this protein were reported to result in sideroblastic anemia and variant nonketotic hyperglycinemia in human. Recently, we have characterized a Chinese congenital sideroblastic anemia patient who has two compound heterozygous missense mutations (c. 301 A>C and c. 443 T>C) in his *GLRX5* gene. Herein, we developed a GLRX5 knockout K562 cell line and studied the biochemical functions of the identified pathogenic mutations and other conserved amino acids with predicted essential functions. We observed that the K101Q mutation (due to c. 301 A>C mutation) may prevent the binding of [Fe-S] to GLRX5 protein, while L148S (due to c. 443 T>C mutation) may interfere with [Fe-S] transfer from GLRX5 to iron regulatory protein 1 (IRP1), mitochondrial aconitase (m-aconitase) and ferrochelatase. We also demonstrated that L148S is functionally complementary to the K51del mutant with respect to Fe/S-ferrochelatase, Fe/S-IRP1, Fe/S-succinate dehydrogenase, and Fe/S-m-aconitase biosynthesis and lipoylation of pyruvate dehydrogenase complex and α-ketoglutarate dehydrogenase complex. Furthermore, we demonstrated that the mutations of highly conserved amino acid residues in GLRX5 protein can have different effects on downstream Fe/S proteins. Collectively, our current work demonstrates that GLRX5 protein is multifunctional in [Fe-S] protein synthesis and maturation and defects of the different amino acids of the protein will lead to distinct effects on downstream Fe/S biosynthesis. J. Cell. Biochem. 117: 207–217, 2016.

KEY WORDS: GLRX5; MUTATIONS; IRON-SULFUR CLUSTER BIOSYNTHESIS

Iron-sulfur clusters [Fe-S] are ancient and versatile inorganic cofactors which participate in electron transfer, catalysis, and multiple regulatory processes [Lill, 2009]. Biogenesis of iron-sulfur proteins in mitochondria involves two main steps. Firstly, an [Fe-S] is transiently assembled on the mitochondrial Isu1 (homolog of ISCU1 in human mitochondria) scaffold protein. The second main step comprises several reactions, including separation of the [Fe-S] from the scaffold protein and [Fe-S] cluster transferred and assembled into apoproteins [Lill et al., 2012].

Glutaredoxin 5 (GLRX5) is a 156 amino acid mitochondrial protein that plays an essential role in mitochondrial [Fe-S] transfer [Lill et al., 2012]. In yeast, it has been demonstrated that Grx5 (yeast homolog of human GLRX5) can specifically interact with the Ssq1-Isu1 complex (yeast counterpart of human HSP70-ISCU1 complex) [Uzarska et al., 2013]. The interaction of Isu1 and Grx5 allows efficient [Fe-S] transfer from Isu1 to Grx5. Deficiencies in GLRX5 cause severe microcytic anemia in zebrafish mutants and congenital sideroblastic anemia (CSA) or variant nonketotic hyperglycinemia (vNKH) in their human counterparts [Wingert et al., 2005; Camaschella et al., 2007; Baker et al., 2014; Liu et al., 2014].

The first reported case of sideroblastic anemia due to GLRX5 deficiency results from a homozygous mutation in the first exon of the *GLRX5* gene that interferes with RNA splicing [Camaschella et al., 2007]. Subsequent mechanistic studies demonstrated that

Grant sponsor: National Basic Research Program of China, MoST 973 program; Grant number: 2012CB934000; Grant sponsor: National Distinguished Youth Scholar Grant of China; Grant number: 31325010.

*Correspondence to: Prof. Guangjun Nie, CAS Key Laboratory for Biomedical Effects of Nanomaterials and Nanosafety, National Center for Nanoscience and Technology, No.11 Zhongguancun Beiyitiao, Beijing 100190, China. E-mail: niegj@nanoctr.cn

Manuscript Received: 21 May 2015; Manuscript Accepted: 17 June 2015

Accepted manuscript online in Wiley Online Library (wileyonlinelibrary.com): 20 June 2015

DOI 10.1002/jcb.25267 • © 2015 Wiley Periodicals, Inc.

decreased GLRX5 levels led to impaired [Fe-S] assembly on iron regulatory protein 1 (IRP1) and ferrochelatase (FECH), the proteins essential for cellular iron homeostasis maintenance and heme biosynthesis, respectively [Ye et al., 2010]. As a result, inhibited heme biosynthesis and cytosolic iron depletion were observed in the patient with the *GLRX5* splicing defect [Camaschella et al., 2007]. No other mutations in GLRX5 have been identified in the subsequent large-scale studies of patients with sideroblastic anemia [Fujiwara and Harigae, 2013]. Recently, we identified a severely affected Chinese CSA patient who is a compound heterozygote for two missense mutations (c. 301 A>C and c. 443 T>C) in the *GLRX5* gene and demonstrated that the two *GLRX5* mutations impair [Fe-S] biogenesis in peripheral blood mononuclear cells (PBMCs) from the proband [Liu et al., 2014].

Apart from CSA, a recent study found that p. K51del and c. 82 ins [GCGTGCGG] mutations in GLRX5 were associated with vNKH in two Lebanese girls and a Chinese boy. Nonketotic hyperglycinemia is caused by deficient glycine cleavage enzyme system [Baker et al., 2014]. Lipoate is an essential cofactor for the glycine cleavage system, pyruvate dehydrogenase (PDH), and α-ketoglutarate dehydrogenase (αKGDH) [Kikuchi et al., 2008]. Biosynthesis of lipoate requires lipoate synthase enzyme (LIAS), which needs an [Fe-S] in a radical S-adenosylmethionine dependent reaction [Baker et al., 2014]. It has been speculated that GLRX5 p. K51del mutation may impair [Fe-S] transfer to LIAS protein, since the mutation was found to cause decreased lipoylation in fibroblast lysate of those vNKH patients [Baker et al., 2014].

Taking together, all the available information from both animal models and human patients point out that GLRX5 plays essential role in various biochemical processes. However, the biochemical functions of the essential amino acids in GLRX5 are still elusive.

In this study, we examine the effects of the all those known pathogenic mutations on [Fe-S] biosynthesis in GLRX5 null K562 cells and demonstrate that L148S (due to c. 443 T>C mutation) is functionally complementary to the K51del mutant with respect to Fe/S-FECH, Fe/S-IRP1, Fe/S- succinate dehydrogenase (SDH, a mitochondrial enzyme which contains three [Fe-S] clusters) and Fe/S-mitochondrial aconitase (m-aconitase) biosynthesis and lipoylation of PDH and αKGDH. Furthermore, we also investigated the biochemical functions of various highly conserved amino acid residues in GLRX5 protein and found that mutations of these residues have distinct effects on Fe/S-FECH, Fe/S-m-aconitase, Fe/S-SDH biosynthesis, and lipoylation of PDH and αKGDH.

MATERIALS AND METHODS

GLRX5 KNOCKOUT K562 CELLS, PLASMID CONSTRUCTION, SITE-DIRECTED MUTAGENESIS, AND TRANSFECTION

Since endogenous GLRX5 protein may somewhat confound the effects of GLRX5 mutants, we used the CRISPR-Cas9 system to develop a stable GLRX5 null K562 cell line in accordance with previous studies [Cong et al., 2013; Ran et al., 2013]. The pLentiCRISPR plasmid was obtained from Addgene. GLRX5 sgRNA was designed by an online CRISPR Design Tool (http://tools.genome-engineering.org, Table I). The GLRX5 sgRNA and a negative control sgRNA (a sgRNA with the scrambled sequence of the GLRX5 sgRNA, Table I) were cloned into pLentiCRISPR plasmid as described previously [Ran et al., 2013]. The resulting plasmid was transfected into K562 cells using an Amaxa Cell Line Nucleofector Kit V (Lonza, Shanghai, China) and Amaxa Nucleofector Device (Lonza, Shanghai, China) in accordance with the manufacturer's protocol. After transfection, the cells were cultured in Iscove's Modified Dubecco's Medium (IMDM) containing 3 μg/mL puromycin for 6 days.

TABLE I. Oligos Used in This Study

Oligos	Sequence(5′→3′)
GLRX5-sgRNAF	CACCGGGCGGAGCAGTTGGACGCGC
GLRX5-sgRNAR	AAACGCGCGTCCAACTGCTCCGCCC
NCsgRNAF	CACCGGCGGAGCAGTTAGGCGCGCG
NCsgRNAR	AAACCGCGCGCCTAACTGCTCCGCC

The mammalian expression vector pcDNA3.1 was obtained from Promega (Madison). Human wild-type *GLRX5* cDNA was isolated from a cDNA library derived from the human cell line HepG2 by PCR and was subsequently cloned into pcDNA3.1 (Promega; Madison) to generate the vector pcDNA3.1-GLRX5-WT. The mutations of interest were introduced via PCR site-directed mutagenesis to generate the vectors pcDNA3.1- GLRX5-K101Q, pcDNA3.1- GLRX5-L148S, pcDNA3.1-GLRX5-K51del, pcDNA3.1-GLRX5-V55P, pcDNA3.1-GLRX5-K59E pcDNA3.1-GLRX5-C67S, pcDNA3.1-GLRX5-R97E, pcDNA3.1-GLRX5-Q111V, pcDNA3.1-GLRX5-F118S, pcDNA3.1-GLRX5-L138P, and pcDNA3.1-GLRX5-K51E. In the event that the CRISPR-Cas9 system could affect the expression of exogenous GLRX5 proteins, we introduced four silent mutations (5′ GGCGGAA-CAATTAGATGCGC 3′; the mutated nucleotides are underlined) into the GLRX5 sgRNA target region of the plasmids to render them non-responsive to the sgRNA. The sequences of the resulting plasmids were verified by direct sequencing. These expression vectors were then transiently transfected into GLRX5 null K562 cells using an Amaxa Cell Line Nucleofector Kit V (Lonza, Shanghai, China) and Nucleofector Device in accordance with the manufacturer's protocol. The transfected cells were studied 48 h after transfection.

ISOLATION OF MITOCHONDRIA, ENZYME ASSAYS, HEME CONTENT ASSAY, AND NONHEME IRON ASSAY

Mitochondrial fractions (MFs) and postmitochondrial fractions (PMFs) of K562 cells, were separated as previously described [Drapier and Hibbs, 1996]. Briefly, 0.007% digitonin was used to lyse cell membrane without affecting the membrane of mitochondria. After centrifuged at 1800*g* for 8 min at 4°C, the supernant was transferred to a pre-cool tube. After this step, more than 95% of mitochondrial material is spun down. Relative aconitase activities of MFs and PMFs were measured by monitoring the disappearance of the ultraviolet (UV) absorbance of *cis*-aconitate in accordance with the same protocol using a UV-5300 Spectrophotometer (Metash, Shanghai, China). Relative mitochondrial PDH, αKGDH and SDH activities were analyzed using the kits from Solarbio (Shanghai, China) in accordance with the manufacturer's protocols using an Infinite M200 multimode reader (TECAN, Grödig, Austria). For heme concentration assay, 10 μg protein sample was added to 0.5 mL of 2.5 M oxalic acid. After heated at 100°C for 30 min, the autofluorescence of protoporphyrin in each sample was measured

with an Infinite M200 plate reader (TECAN, Grödig, Austria) at an excitation wavelength of 400 nm and an emission wavelength of 620 nm. Samples without heating were used to correct for background autofluorescence of endogenous protoporphyrin. Cellular, cytosolic and mitochondrial nonheme iron levels were determined using a QuantiChrom Iron Assay Kit (BioAssay System, California) and were normalized to protein content, which was measured using BCA method (Solarbio, Beijing, China).

IMMUNOBLOTTING, CO-IMMUNOPRECIPITATION, AND NONDENATURING GEL ELECTROPHORESIS

Transfected K562 cells were lysed with RIPA buffer (Solarbio, Beijing, China) containing 1 mM PMSF (Solarbio, Beijing, China). Protein samples (40–80 μg) were electrophoresed on 10–12% sodium dodecyl sulfate–polyacrylamide gels. Loading and transfer were then confirmed by Ponceau red staining. The proteins were then transferred onto a polyvinylidene fluoride (PVDF) membrane. After preincubation in blocking solution at room temperature, the PVDF membrane was incubated with the appropriate antibodies for 2–3 hours at room temperature. After washing 3 times with TBST for 5 min each time, the membrane was incubated for 1 h with a secondary antibody linked to horseradish peroxidase (goat anti-rabbit IgG, donkey anti-goat or goat anti-mouse IgG, 1/10000, Santa Cruz Biotechnology, Santa Cruz). After washing 3 times with TBST for 5 min each time, immunoreactive proteins were visualized using SuperSignal West Pico Chemiluminescent Substrate (Thermo Scientific, Rockford). For nondenaturing gel electrophoresis, 30 μg of total protein was separated by using a native 10% polyacrylamide gel [Campanella et al., 2004]. For co-immunoprecipitation of ISCU1-GLRX5 complexes, anti-ISCU1 antibodies were added to the MFs of transfected GLRX5 KO K562 cells and incubated for 2 h at 4°C. Then Protein A-agarose beads (Santa Cruz Biotechnology, Santa Cruz) were used to collect antigen-antibody complexes. Afterwards, GLRX5 proteins were detected in the precipitates by western blotting.

Primary antibodies used in this study were raised against TfR1 (Invitrogen, Shanghai, China), H-ferritin (Alpha Diagnostic, San Antonio), GAPDH (Abcam, Cambridge, UK), IRP1 (Abcam, Cambridge, UK), GLRX5 (Lifespan biosciences), FECH (Santa Cruz Biotechnology, Santa Cruz), ISCU1 (Santa Cruz Biotechnology, Santa Cruz) and COX IV (Abcam, Cambridge, UK).

GLRX5 PURIFICATION AND ANAEROBIC [Fe-S] RECONSTITUTION

The pET30a-His-GLRX5-WT, pET30a-His-GLRX5-L148S, and pET30a-His-GLRX5-K101Q expression vectors were constructed by cloning mature wild-type and mutated N-terminal His6 tagged human GLRX5 sequences into the pET30a vector (Novagen, Darmstadt, Germany). His-tagged GLRX5 proteins were expressed and purified through the technical services of Huada Protein (Beijing, China). After incubation for 2.5 h in a reconstitution mix containing 100 μM GLRX5 protein, 5 mM DTT, 4 mM GSH, 2 mM lithium sulfide, and 3 mM ferrous chloride under anerobic conditions in a glove box, [Fe-S] clusters were reconstituted into purified GLRX5 proteins as described [Ye et al., 2010]. Reconstituted proteins were then purified by sequential passage through a PD-10 desalting column and a HiTrap Q HP column (GE Healthcare, Beijing, China). All purification buffers contained 2 mM GSH (Sigma–Aldrich, Shanghai, China). An Amicon Ultra Centrifugal Filter Device (Millipore, Billerica, MA) was used to concentrate the recovered proteins. UV-vis spectrophotometry of holo-GLRX5 was performed using a UV-5300 Spectrophotometer (Metash, Shanghai, China).

STATISTICAL ANALYSIS

Results are expressed as mean ± SD of three independent experiments. Two-tailed Student's *t* test was used to determine the *P* value. A *P* value of less than 0.05 was considered significant (*), while a *P* value of less than 0.01 was considered very significant (**).

RESULTS

[Fe-S] CLUSTER BIOSYNTHESIS IS DISTURBED BY THE K101Q AND L148S MUTANTS IN K562 CELLS

To investigate the effects of K101Q and L148S mutants on [Fe-S] biogenesis, we developed a GLRX5 null human K562 cell line using the CRISPR-Cas9 system [Cong et al., 2013; Ran et al., 2013]. As shown in Figure 1A, GLRX5 protein decreased to almost undetectable levels in K562 cells transfected with pLentiCRISPR-GLRX5 sgRNA. These GLRX5 null K562 cells have significantly decreased heme content (Fig. 1B), consistent with previous work on the effects of GLRX5 on cellular heme levels [Ye et al., 2010]. Since there is still some heme in GLRX5 null K562 cells, we speculate that other pathways were involved in the biosynthesis of Fe/S cluster. Furthermore, GLRX5 null K562 cells have increased mitochondrial nonheme iron levels, while their cytosolic nonheme iron levels are similar to that of control cells (Fig. 1C).

GLRX5 null K562 cells were then transfected with pcDNA3.1 expression plasmids carrying either the wild-type *GLRX5* gene, one of the two mutated *GLRX5* sequences, or the two mutated plasmids together. The expression levels of exogenous GLRX5 proteins were significantly higher than that of endogenous GLRX5 in K562 cells (Figure S1). Neither of the mutations significantly influenced the amount of GLRX5 protein imported into the mitochondria as western blotting for mitochondrial GLRX5 showed similar levels for both the mutant and wild-type proteins (Fig. 2A, Figure S1A). GLRX5 was nearly undetectable in PMFs of untransfected nor transfected cells (data not shown). Nondenaturing gel electrophoresis showed that Fe/S-IRP1 levels were reduced in GLRX5 null cells and in K562 cells expressing the K101Q, L148S, and K101Q/L148S mutants relative to wild-type GLRX5 (Fig. 2B). Fe/S-IRP1 possesses cytosolic aconitase (c-aconitase) activity. We thus investigated the c-aconitase activity in these cells. Cytosolic aconitase activity was significantly lower in GLRX5 null K562 cells than in control cells (Fig. 2C). A significantly higher c-aconitase activity was observed in K562 cells expressing GLRX5-WT relative to control cells, while the c-aconitase activity was not rescued by either GLRX5 mutant or their combination (Fig. 2C). In accordance with these observations, in GLRX5 null and mutant expressing K562 cells, significantly increased levels of TfR1 and decreased levels of H-ferritin were observed (Fig. 2A, Figure S1B and C). Based on these observations, and given that cellular nonheme iron levels were not reduced in K562 cells expressing GLRX5 mutants relative to wild-type GLRX5 (Fig. 2E and F), we concluded

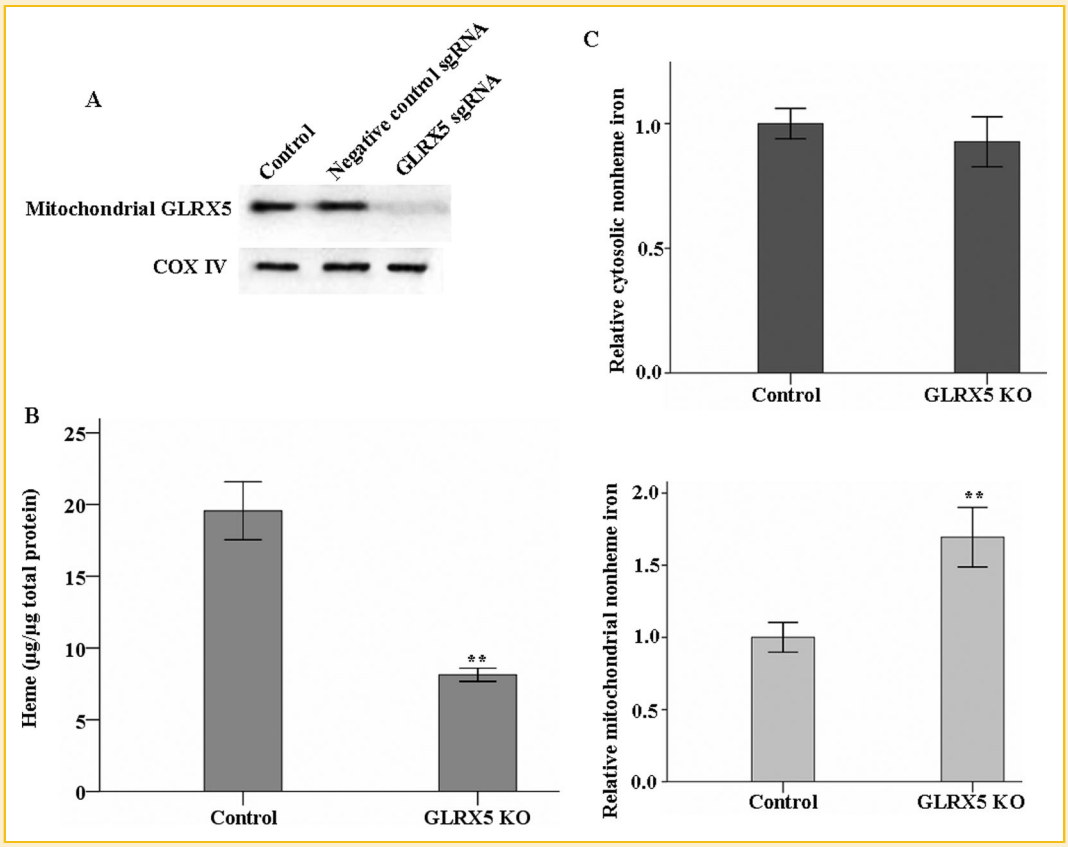

Fig. 1. Characterization of the GLRX5 null K562 cell line. (A) Western blotting of mitochondrial GLRX5 in control K562 cells (untreated K562 cells), K562 cells transfected with pLentiCRISPR-negative control sgRNA and K562 cells transfected with pLentiCRISPR-GLRX5 sgRNA. Equal loading was confirmed by showing that COX IV levels were unchanged. (B) Heme content analysis in control and GLRX5 KO K562 cells. (C) Relative cytosolic (upper panel) and mitochondrial (lower panel) nonheme iron levels (results expressed as the mean percentage of the nonheme iron content in control cells).

that the low levels of Fe/S-IRP1 protein result from impaired cytosolic [Fe-S] assembly rather than from limited iron availability.

We next investigated whether these GLRX5 mutations could influence [Fe-S] cluster biogenesis in mitochondria using aconitase activity as a marker. A significant reduction in m-aconitase activity was observed in GLRX5 null as well as in mutants expressing cells (Fig. 2D). These results indicate that [Fe-S] cluster biosynthesis in the MFs and PMFs of K562 cells was disturbed by the two mutations. In support of this conclusion, FECH levels, evaluated in GLRX5 null K562 cells and K562 cells expressing GLRX5 mutants, were found to be significantly decreased (Fig. 2A, Figure S1D). FECH expression is not regulated by the iron regulatory protein-iron responsive element (IRP-IRE) system and its posttranslational stability is dependent on [Fe-S] availability [Crooks et al., 2010] and it was shown that GLRX5 may function as a specific [2Fe-2S] donor to FECH [Ye et al., 2010].

THE K101Q MUTATION BLOCKS [Fe-S] ANAEROBIC RECONSTITUTION IN VITRO

It has been suggested that GLRX5 can bind an iron-sulfur cluster in vitro [Ye et al., 2010] and we confirmed this using UV spectrophotometry by showing that wild-type GLRX5 protein showed an A_{280} absorption peak, and a shoulder between 300 and 350 nm before anaerobic reconstitution (Fig. 3A), and significant absorption peaks at 330 nm and 420 nm after reconstitution (Fig. 3B). Before reconstitution, the L148S and K101Q GLRX5 proteins showed only the 280 nm absorption peak (Fig. 3C and E). After anaerobic reconstitution, the L148S mutant showed similar peaks to wild-type protein (Fig. 3D), while the K101Q mutant showed only the 300–350 nm shoulder (Fig. 3F). Given that biological [2Fe-2S] typically show absorption peaks around 330 nm and 420–460 nm [Fu et al., 1994], these results suggest that a [2Fe-2S] can be reconstituted in both wild-type GLRX5 and the L148S mutant, while the K101Q mutation abolishes [Fe-S] reconstitution.

GLRX5 DIRECTLY INTERACTS WITH ISCU IN K562 CELLS

As we mentioned above, a previous study has demonstrated that GLRX5 can specifically interact with the Ssq1-Isu1 complex in yeast [Uzarska et al., 2013]. Therefore, we performed co-immunoprecipitation experiments in K562 cells expressing WT and mutated GLRX5 to investigate whether GLRX5 could interact with ISCU scaffold in human cells. After cellular extracts were immunoprecipitated with an anti-ISCU1 antibody and subjected to western blotting, GLRX5 protein could be detected in the extracts

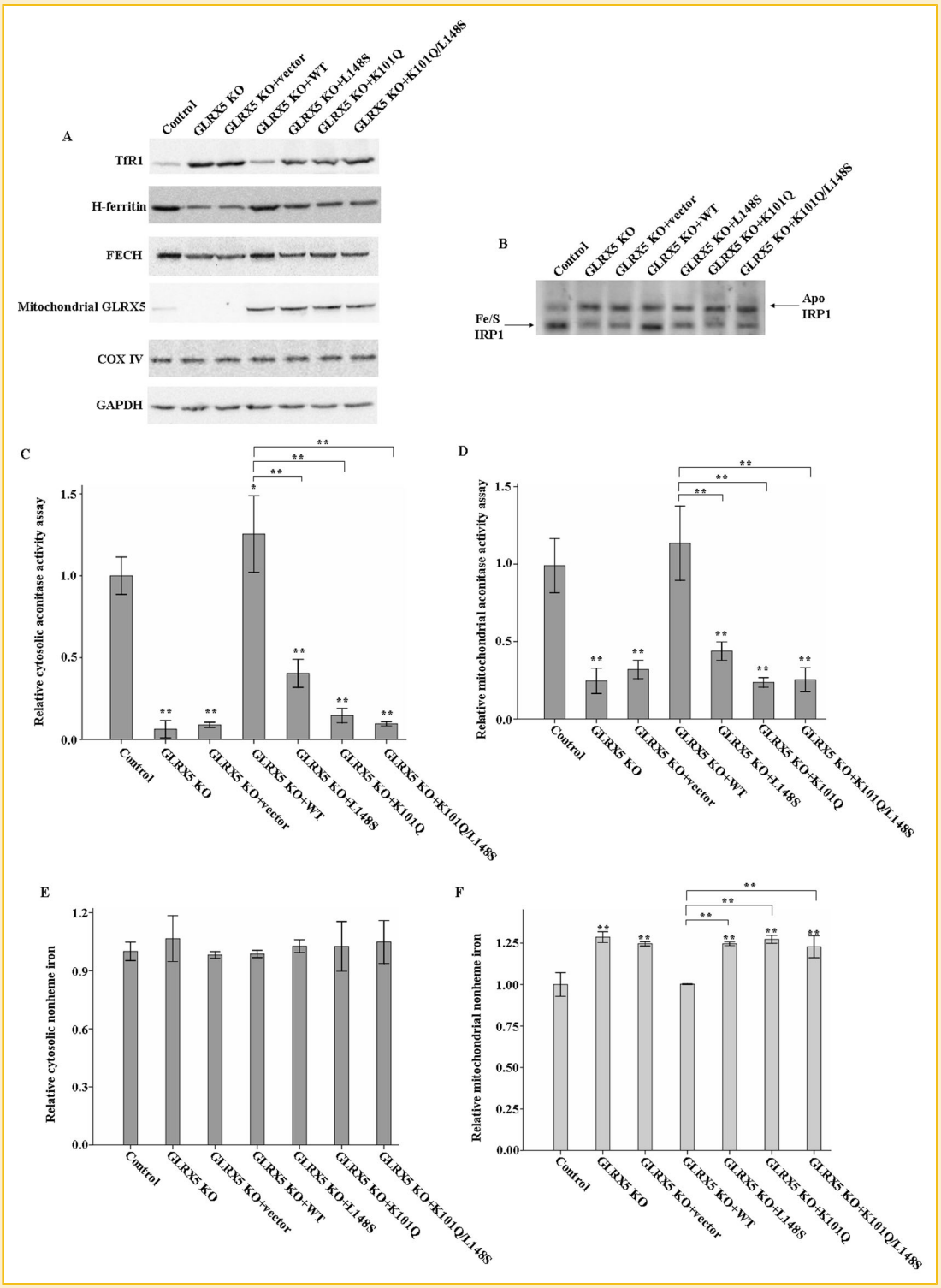

Fig. 2. Functional analysis of exogenous wild-type GLRX5 (WT), the L148S mutant, the K101Q mutant and a combination of the two mutations (K101Q/L148S) in GLRX5 null K562 cells. (A) Western blotting of TfR1, H-ferritin, FECH and mitochondrial GLRX5. Equal loading was confirmed by showing that COX IV and GAPDH levels were unchanged. (B) Determination of IRP1 status by immunoblotting of proteins separated by native PAGE. Relative cytosolic (C) and mitochondrial (D) aconitase activity assay (results expressed as the mean percentage of the aconitase activity in control cells). Comparison of relative aconitase activities between GLRX5 KO + WT and GLRX5 KO + L148S groups, GLRX5 KO+K101Q groups and GLRX5 KO + K101Q/L148S groups, respectively, showed significantly decreased relative aconitase activities in K562 cells expressing GLRX5 mutants. Relative cytosolic (E) and mitochondrial (F) nonheme iron levels (results expressed as the mean percentage of the nonheme iron content in control cells). Comparison of relative cytosolic nonheme iron levels between GLRX5 KO + WT and GLRX5 KO + L148S groups, GLRX5 KO + K101Q groups and GLRX5 KO + K101Q/L148S groups, respectively, showed significantly increased cytosolic nonheme iron levels in K562 cells expressing GLRX5 mutants.

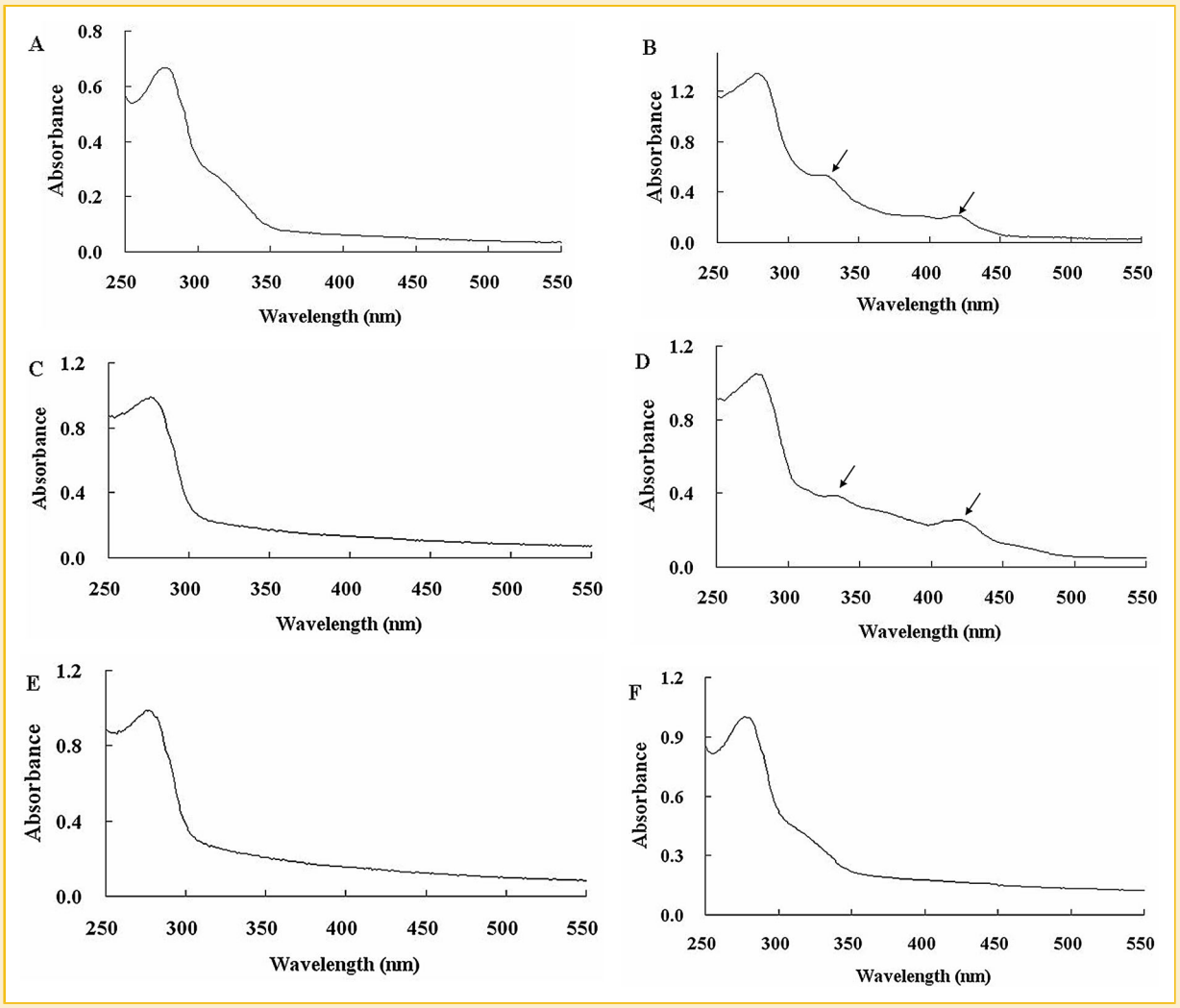

Fig. 3. In vitro [2Fe-2S] cluster reconstitution. (A, C and E) UV-vis spectrophotometry of wild-type GLRX5 protein and the L148S and K101Q mutants before reconstitution. (B, D and F) UV-vis spectrophotometry of wild-type GLRX5 protein and the L148S and K101Q mutants after reconstitution. Arrows indicate absorption peaks of biological [2Fe-2S] clusters at 330 nm and 420 nm.

(Fig. 4A). Equal amounts of GLRX5-ISCU1 complex were observed in K562 transfected with WT or mutated *GLRX5* (Fig. 4A), suggesting that neither of the mutations affects GLRX5-ISCU1 interaction in transfected K562 cells.

THE K101Q AND L148S SUBSTITUTIONS HAVE DIFFERENT EFFECTS ON MITOCHONDRIAL PDH AND αKGDH ACTIVITIES

The p. K51del and c. 82ins[GCGTGCGG] GLRX5 mutations identified in variant NKH patients can lead to decreased lipoylation, which consequently results in a decrease in the activities of PDH and αKGDH [Baker et al., 2014]. We thus tested whether PDH and αKGDH activities were affected by the K101Q and L148S mutations in K562 cells. Interestingly, we observed a significant reduction in PDH and αKGDH activities only in GLRX5 null and K101Q mutant expressing K562 cells, while in the cells expressing the L148S and K101Q/L148S mutants αKGDH and PDH activities were not reduced (Fig. 5A and B).

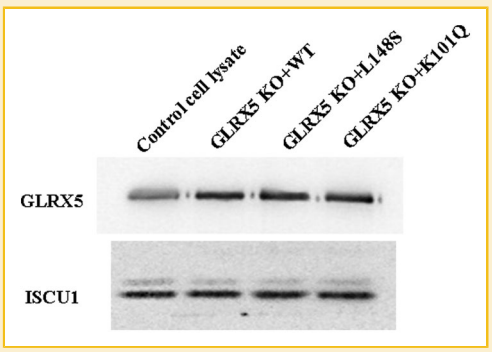

Fig. 4. GLRX5-ISCU interaction analysis. Extracts of untransfected or transfected K562 cells were immunoprecipitated using an anti-ISCU1 antibody, then subjected to western blotting using an antibody against GLRX5 (upper panel). The lower panel shows western blotting of cellular extracts for ISCU1.

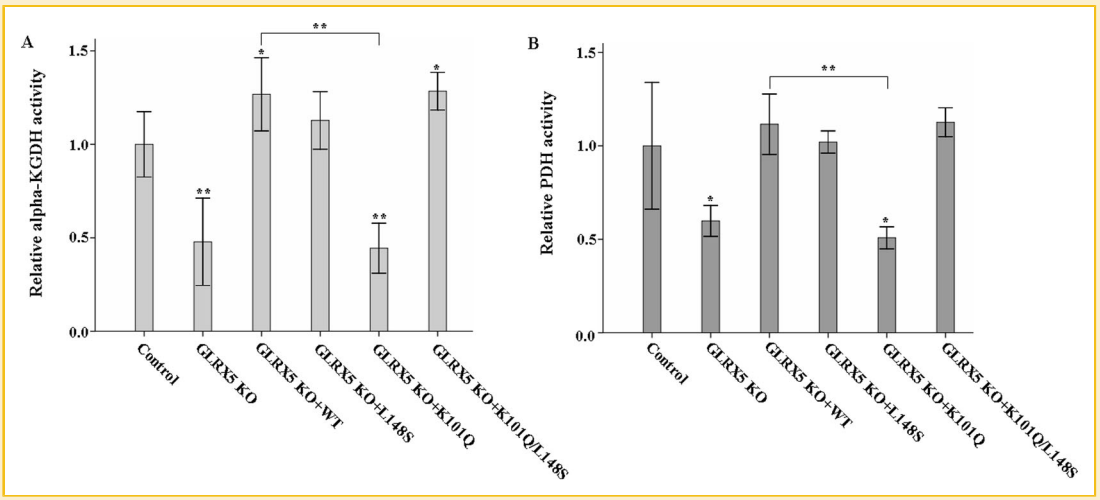

Fig. 5. αKGDH and PDH activity assays. (A) Relative αKGDH complex activity was significantly reduced in GLRX5 KO and K101Q mutant-expressing K562 cells. Results are expressed as the mean percentage of the αKGDH complex activity in control cells. (B) Relative PDH complex activity was significantly reduced in GLRX5 KO and K101Q mutant-expressing K562 cells. Results expressed as the mean percentage of the PDH complex activity in control cells. Comparison of relative αKGDH and PDH activities between GLRX5 KO+WT and GLRX5 KO+K101Q groups showed significant decreased αKGDH and PDH activities in K101Q mutant-expressing K562 cells.

FUNCTIONAL COMPLEMENTATION OF THE GLRX5 MUTANTS IN GLRX5 NULL K562 CELLS

To test whether the L148S and K101Q mutants are functionally complementary to the K51del mutant, we investigated FECH expression level and performed aconitase, PDH, αKGDH and SDH activity assays in K562 cells expressing K51del, L148S/K51del and K101Q/K51del mutants. As shown in Fig. 6, there was no significant difference in the FECH expression level and aconitase activities among K562 cells expressing WT or mutated GLRX5 proteins. Given that GLRX5 is a haplosufficient gene, this suggests that the K51del mutant could rescue the FECH expression and aconitase activities in L148S and K101Q mutant expressing K562 cells. Significant reductions in PDH and αKGDH activities were observed in K562 cells expressing K51del and K101Q/K51del mutants, while in K562 cells expressing the L148S/K51del mutants, αKGDH and PDH activities were not reduced (Fig. 6D and E). This suggests that the L148S mutant, but not the K101Q mutant, is functionally complementary to the K51del mutant with respect to lipoate biosynthesis. Furthermore, according to Figure 6F, significant reduction in SDH activities were observed in K101Q, K51del, and K101Q/K51del mutant expressing cells but not in L148S or L148S/K51del mutant expressing cells. This indicates that L148S mutant could rescue SDH activity in K562 cells expressing K51del mutant.

FUNCTIONAL ANALYSIS OF HIGHLY CONSERVED GLRX5 AMINO-ACID RESIDUES IN GLRX5 NULL K562 CELLS

To investigate whether mutations of different amino acid residues in GLRX5 protein have diverse impact on downstream Fe/S proteins, we introduced seven missense mutations (V55P, K59E, C67S, R97E, Q111V, F118S, and L138P) to human GLRX5 protein. Each of these mutations affects a GLRX5 residue that is highly conserved from yeast to human. We also generated a K51E mutant to compare its biochemical functions with those of K51del. Protein levels of FECH and m-aconitase, PDH, αKGDH, and SDH activities were determined in K562 cells expressing these mutants. As shown in Figure 7, significantly decreased levels of FECH were observed in K562 cells expressing the aforementioned mutants. Significant reduction in m-aconitase activities were observed in V55P, K59E, C67S, R97E, Q111V, F118S, and L138P mutant expressing cells but not in K51E mutant expressing cells. K562 cells expressing K59E, C67S, R97E, Q111V, F118S, and L138P mutants have significantly reduced PDH, αKGDH and SDH activities, while there was no significant difference in PDH, αKGDH, and SDH activities among K562 cells expressing WT, V55P, or K51E GLRX5 proteins.

DISCUSSION

Iron-sulfur [Fe-S] clusters are ubiquitous prosthetic groups that are associated with a wide range of biochemical processes [Lill, 2009]. Defects in the [Fe-S] biosynthesis machinery are responsible for a series of human diseases, such as Friedreich ataxia, myopathy with ISCU deficiency, CSA and vNKH [Rouault and Tong, 2008]. In GLRX5-deficient erythroblasts, mitochondrial [Fe-S] biosynthesis is blocked, thus activating the IRE binding activity of IRP1, which suppresses the expression of ALA synthase 2 (ALAS2) [Ponka, 1997]. This in turn impairs the heme biosynthetic pathway and reduces iron utilization for this pathway and iron accumulation. Meanwhile, the lack of [Fe-S] also causes the degradation of FECH and this compounds the impairment of the heme biosynthetic pathway [Ponka, 1997]. In GLRX5-deficient non-erythroid cells, however, the lack of [Fe-S] is likely better tolerated, since the ubiquitous form of ALAS (ALAS1) is not regulated by IRP-IRE system and less FECH is required in these cells to synthesize heme [Ye et al., 2010]. In the first reported case of GLRX5 deficiency in a CSA patient, a quantitative reduction in the level of GLRX5, due to a homozygous splicing defect in *GLRX5*, led to sideroblastic anemia through impaired [Fe-S]

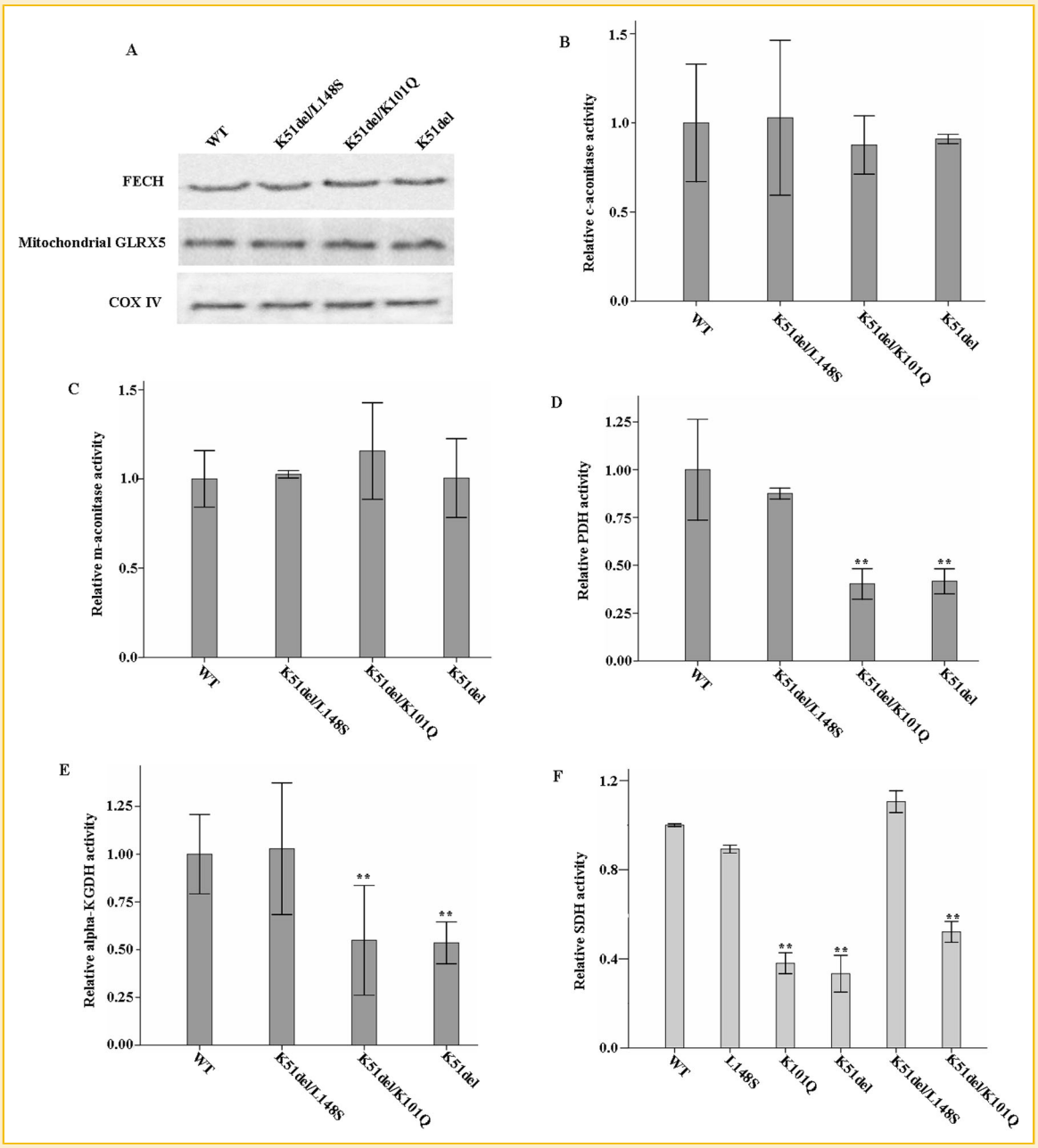

Fig. 6. Functional complementation studies of the GLRX5 mutants in GLRX5 null K562 cells. (A) Western blotting of FECH and mitochondrial GLRX5. Equal loading was confirmed by showing that COX IV level was unchanged. (B, C) Relative cytosolic (B) and mitochondrial (C) aconitase activity assay (results expressed as the mean percentage of the aconitase activity in K562 cells expressing WT GLRX5 proteins). (D, E) Relative PDH (D) and αKGDH (E) complex activity was significantly reduced in K51del/K101Q mutant-expressing K562 cells. Results are expressed as the mean percentage of the αKGDH and PDH complex activity in WT GLRX5-expressing K562 cells. (F) Relative SDH activity assay (results expressed as the mean percentage of the SDH activity in K562 cells expressing WT GLRX5 proteins).

biogenesis [Camaschella et al., 2007]. However, deletion and insertion mutations in *GLRX5* have been associated with vNKH, suggesting that the nature of the *GLRX5* mutation has a considerable bearing on the clinical phenotype [Baker et al., 2014].

In this study, we firstly examined the effects of the identified GLRX5 mutations on [Fe-S] biosynthesis. Since no adequate in vivo erythroid material was available, functional studies of the two *GLRX5* missense mutations were carried out in GLRX5 null human erythroleukemia K562 cells transfected with GLRX5 expressing plasmids.

Disrupted cytosolic and mitochondrial [Fe-S] cluster biosynthesis was evident in GLRX5 null K562 cells transfected with plasmids expressing exogenous GLRX5 mutants. A previous study demonstrated that a tetrameric organization of GLRX5 is required for its

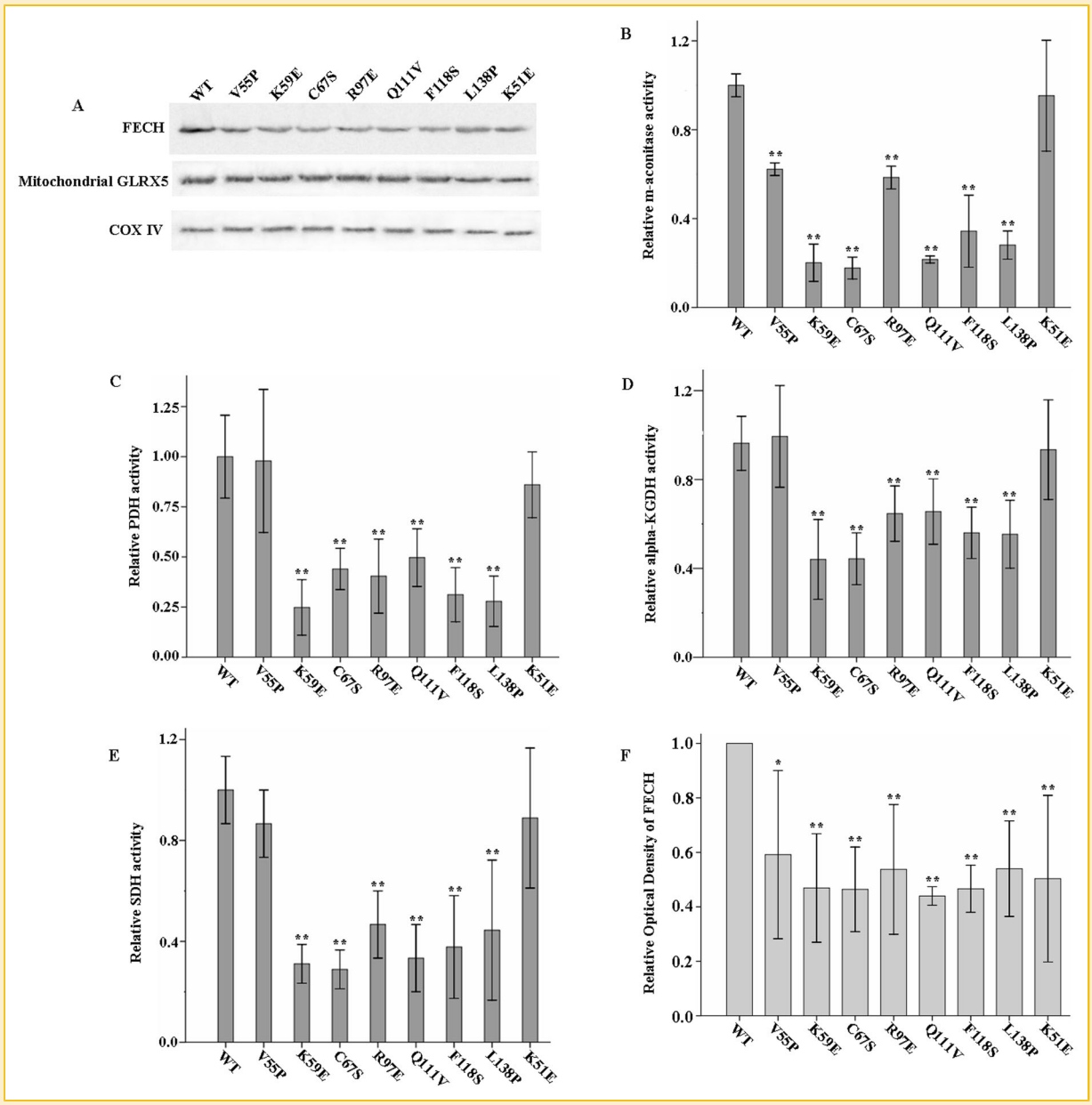

Fig. 7. Functional analysis of highly conserved GLRX5 amino acid residues in GLRX5 null K562 cells. (A) Western blotting of FECH and mitochondrial GLRX5. Equal loading was confirmed by showing that COX IV level was unchanged. (B) Relative mitochondrial aconitase activity assay (results expressed as the mean percentage of the aconitase activity in K562 cells expressing WT GLRX5 proteins). (C, D) Relative PDH (C) and αKGDH (D) complex activity analysis. Results are expressed as the mean percentage of the αKGDH and PDH complex activity in WT GLRX5-expressing K562 cells. (E) Relative SDH activity assay (results expressed as the mean percentage of the SDH activity in K562 cells expressing WT GLRX5 proteins). (F) Relative optical density of FECH in Figure 7A. Results are expressed as the mean percentage of the optical density of the band in control lane.

[Fe-S] integration. Each [2Fe-2S] cluster is ligated by Cys67 thiols contributed by two GLRX5 protomers and two cysteine thiols from two glutathione (GSH) [Johansson et al., 2011]. Lys101 in the GLRX5 protein is important for its interaction with GSH. The glycine carboxylate of GSH has ionic interactions with the side chains of Lys59, Arg97 and Lys101 of crystallized human GLRX5 [Johansson et al., 2011]. Since the K59Q substitution abolishes [Fe-S] reconstitution in vitro [Ye et al., 2010], we speculated that the K101Q mutation could also interfere with the interaction between GLRX5 and iron-sulfur clusters. To test this hypothesis, we performed in vitro anaerobic [Fe-S] reconstitution studies. These experiments indicated that the K101Q mutation does impair the reconstitution of [Fe-S] in vitro, as predicted.

GLRX5 plays a major role in mitochondrial [Fe-S] transfer to apoproteins. In yeast, Grx5 specifically interacts with the Ssq1-Isu1 complex [Uzarska et al., 2013]. In this study, we have demonstrated that there is a physical interaction between GLRX5 and ISCU in human K562 cells, and that this interaction is not

affected by K101Q and L148S mutations. This observation confirms that the function of GLRX5 is conserved from yeast to higher eukaryotes.

In addition to the aforementioned functional characterizations of the previously identified GLRX5 mutations, we also found that, while GLRX5 null K562 cells and K562 cells expressing mutant K101 had significantly reduced PDH and αKGDH activities, those expressing the L148S and L148S/K101Q mutants did not. Consistent with these findings, the previously described CSA patient who is heterozygous for K101Q and L148S mutations does not have phenotypic features of vNKH [Liu et al., 2014]. Given that GLRX5 is a haplosufficient gene, these phenomena indicate that the L148S mutation can lead to decreased Fe/S-IRP1, Fe/S-m-aconitase and Fe/S-FECH levels without affecting lipoylation in human cells. Consistent with this conclusion, the L148S mutant is functionally complementary to the K51del mutant in terms of Fe/S-IRP1, Fe/S-m-aconitase, Fe/S-FECH and lipoate biosynthesis and that the patients with the p.K51del mutation in GLRX5 who do not have sideroblastic anemia, have normal cytosolic and mitochondrial aconitase activity [Baker et al., 2014]. Another interesting finding is that L148S mutant could also rescue the SDH activity in K562 cells expressing K51del mutants. Taken together, functional complementation between the GLRX5 mutants indicates that mutations of different amino acid residues in GLRX5 protein have diverse impacts on downstream Fe/S proteins.

In order to test this hypothesis, we introduced seven missense mutations to human GLRX5 protein and investigated their biochemical functions. Indeed, we observed that the all the GLRX5 mutants examined, except V55P and K51E, interfere with lipoate and Fe/S-SDH biosynthesis. Additionally, the K51E and K51del mutants have different impacts on the biosynthesis of lipoate, Fe/S-m-aconitase, Fe/S-FECH and Fe/S-SDH. Taken together, these results demonstrate that GLRX5 is a multifunctional protein and defects of different residues in GLRX5 have diverse impacts on downstream Fe/S proteins. Furthermore, since all the investigated GLRX5 mutants result in decreased FECH level, we speculate that heme biosynthesis pathway is more vulnerable to GLRX5 dysfunction in humans than other metabolic pathways. Consistent with this speculation, both our patient and the patient with a GLRX5 splicing defect develop exclusively sideroblastic anemia [Camaschella et al., 2007; Liu et al., 2014].

In conclusion, we demonstrated that functional defects in the GLRX5 protein can interfere with the biosynthesis of [Fe-S] clusters, and thereby leading to a CSA phenotype. Furthermore, according to previous studies and our own results, defects of different amino acids in GLRX5 protein could have different effects on human cells, thus provides further insights into the biochemical function of human GLRX5.

ACKNOWLEDGMENT

This work was supported by the grant from the National Basic Research Program of China, MoST 973 program (2012CB934000, G.N.) and the National Distinguished Youth Scholar Grant of China (31325010, G.N.). G.N. also gratefully acknowledges the support of the Chinese Academy of Sciences Hundred Talents Program. G.J.A. is a Senior Research Fellow of the National Health and Medical Research Council of Australia and a recipient of Senior Visiting Professorship of CAS.

REFERENCES

Baker PR, Friederich MW, Swanson MA, Shaikh T, Bhattacharya K, Scharer GH, Aicher J, Creadon-Swindell G, Geiger E, MacLean KN, Lee WT, Deshpande C, Freckmann ML, Shih LY, Wasserstein M, Rasmussen MB, Lund AM, Procopis P, Cameron JM, Robinson BH, Brown GK, Brown RM, Compton AG, Dieckmann CL, Collard R, Coughlin CR, 2nd, Spector E, Wempe MF, Van Hove JL. 2014. Variant non ketotic hyperglycinemia is caused by mutations in LIAS, BOLA3 and the novel gene GL RX5. Brain 137:366–379.

Camaschella C, Campanella A, De Falco L, Boschetto L, Merlini R, Silvestri L, Levi S, Iolascon A. 2007. The human counterpart of zebrafish shiraz shows sideroblastic-like microcytic anemia and iron overload. Blood 110: 1353–1358.

Campanella A, Levi S, Cairo G, Biasiotto G, Arosio P. 2004. Blotting analysis of native IR P1: A novel approach to distinguish the different forms of IRP1 in cells and tissues. Biochemistry 43:195–204.

Cong L, Ran FA, Cox D, Lin S, Barretto R, Habib N, Hsu PD, Wu X, Jiang W, Marraffini LA, Zhang F. 2013. Multiplex genome engineering using CRISPR/Cas systems. Science 339:819–823.

Crooks DR, Ghosh MC, Haller RG, Tong WH, Rouault TA. 2010. Posttranslational stability of the heme biosynthetic enzyme ferrochelatase is dependent on iron availability and intact iron-sulfur cluster assembly machinery. Blood 115:860–869.

Drapier JC, Hibbs JB, Jr. 1996. Aconitases: A class of metalloproteins highly sensitive to nitric oxide synthesis. Methods Enzymol 269:26–36.

Fu W, Jack RF, Morgan TV, Dean DR, Johnson MK. 1994. NifU gene product from Azotobacter vinelandii is a homodimer that contains two identical [2Fe-2S] clusters. Biochemistry 33:13455–13463.

Fujiwara T, Harigae H. 2013. Pathophysiology and genetic mutations in congenital sideroblastic anemia. Pediatr Int 55:675–679.

Johansson C, Roos AK, Montano SJ, Sengupta R, Filippakopoulos P, Guo K, von Delft F, Holmgren A, Oppermann U, Kavanagh KL. 2011. The crystal structure of human GLR X5: iron–sulfur cluster co–ordination, tetrameric assembly and monomer activity. Biochem J 433:303–311.

Kikuchi G, Motokawa Y, Yoshida T, Hiraga K. 2008. Glycine cleavage system: Reaction mechanism, physiological significance, and hyperglycinemia. Proc Jpn Acad Ser B Phys Biol Sci 84:246–263.

Lill R 2009. Function and biogenesis of iron-sulphur proteins. Nature 460:831–838.

Lill R, Hoffmann B, Molik S, Pierik AJ, Rietzschel N, Stehling O, Uzarska MA, Webert H, Wilbrecht C, Muhlenhoff U. 2012. The role of mitochondria in cellular iron-sulfur protein biogenesis and iron metabolism. Biochim Biophys Acta 1823:1491–1508.

Liu G, Guo S, Anderson GJ, Camaschella C, Han B, Nie G. 2014. Heterozygous missense mutations in the GLRX5 gene cause sideroblastic anemia in a Chinese patient. Blood 124:2750–2751.

Ponka P 1997. Tissue-specific regulation of iron metabolism and heme synthesis: Distinct control mechanisms in erythroid cells. Blood 89:1–25.

Ran FA, Hsu PD, Wright J, Agarwala V, Scott DA, Zhang F. 2013. Genome engineering using the CRISPR-Cas9 system. Nat Protoc 8:2281–2308.

Rouault TA, Tong WH. 2008. Iron-sulfur cluster biogenesis and human disease. Trends Genet 24:398–407.

Uzarska MA, Dutkiewicz R, Freibert SA, Lill R, Muhlenhoff U. 2013. The mitochondrial Hsp70 chaperone Ssq1 facilitates Fe/S cluster transfer from Isu1 to Grx5 by complex formation. Mol Biol Cell 24:1830–1841.

Wingert RA, Galloway JL, Barut B, Foott H, Fraenkel P, Axe JL, Weber GJ, Dooley K, Davidson AJ, Schmid B, Paw BH, Shaw GC, Kingsley P, Palis J, Schubert H, Chen O, Kaplan J, Zon LI. 2005. Deficiency of glutaredoxin 5 reveals Fe-S clusters are required for vertebrate haem synthesis. Nature 436:1035–1039.

Ye H, Jeong SY, Ghosh MC, Kovtunovych G, Silvestri L, Ortillo D, Uchida N, Tisdale J, Camaschella C, Rouault TA. 2010. Glutaredoxin 5 deficiency causes sideroblastic anemia by specifically impairing heme biosynthesis and depleting cytosolic iron in human erythroblasts. J Clin Invest 120: 1749–1761.

SUPPORTING INFORMATION

Additional supporting information may be found in the online version of this article at the publisher's web-site.